

## Supporting information

Xiang Di<sup>a</sup>, Jian Li<sup>a</sup>, Mingming Yang<sup>a</sup>, Qian Zhao<sup>a</sup>, Guolin Wu<sup>a,\*</sup>, Pingchuan Sun<sup>a,\*</sup>

Key Laboratory of Functional Polymer Materials, Institute of Polymer Chemistry,

College of Chemistry, Nankai University, Tianjin 300071, P. R. China.

E-mail: guolinwu@nankai.edu.cn; Fax: +86 22 23502749; Tel: +86 22 23507746

**Table S1. Recipes for all hydrogels**

<b>Samples</b>	<b>LiCl (g)</b>	<b>SDS (g)</b>	<b>AM (mmol)</b>	<b>BA-A (mmol)</b>	<b>ACG (mmol)</b>	<b>KPS (mg)</b>	<b>Water (mL)</b>
<b>PAM-ACG</b>	0.0	0.0	60	0.0	12	40	10
<b>PAM-BA-A-0.0</b>	0.4	0.8	60	0.0	12	40	10
<b>PAM-BA-A-0.5</b>	0.4	0.8	60	0.5	12	40	10
<b>PAM-BA-A-1.0</b>	0.4	0.8	60	1.0	12	40	10
<b>PAM-BA-A-1.5</b>	0.4	0.8	60	1.5	12	40	10
<b>PAM-BA-A-2.0</b>	0.4	0.8	60	2.0	12	40	10
<b>PAM-BA-A-ACG-0</b>	0.4	0.8	60	1.5	0	40	10
<b>PAM-BA-A-ACG-3</b>	0.4	0.8	60	1.5	3	40	10
<b>PAM-BA-A-ACG-6</b>	0.4	0.8	60	1.5	6	40	10
<b>PAM-BA-A-ACG-12</b>	0.4	0.8	60	1.5	12	40	10
<b>PAM-BA-A-ACG-</b>	0.4	0.8	60	1.5	15	40	10

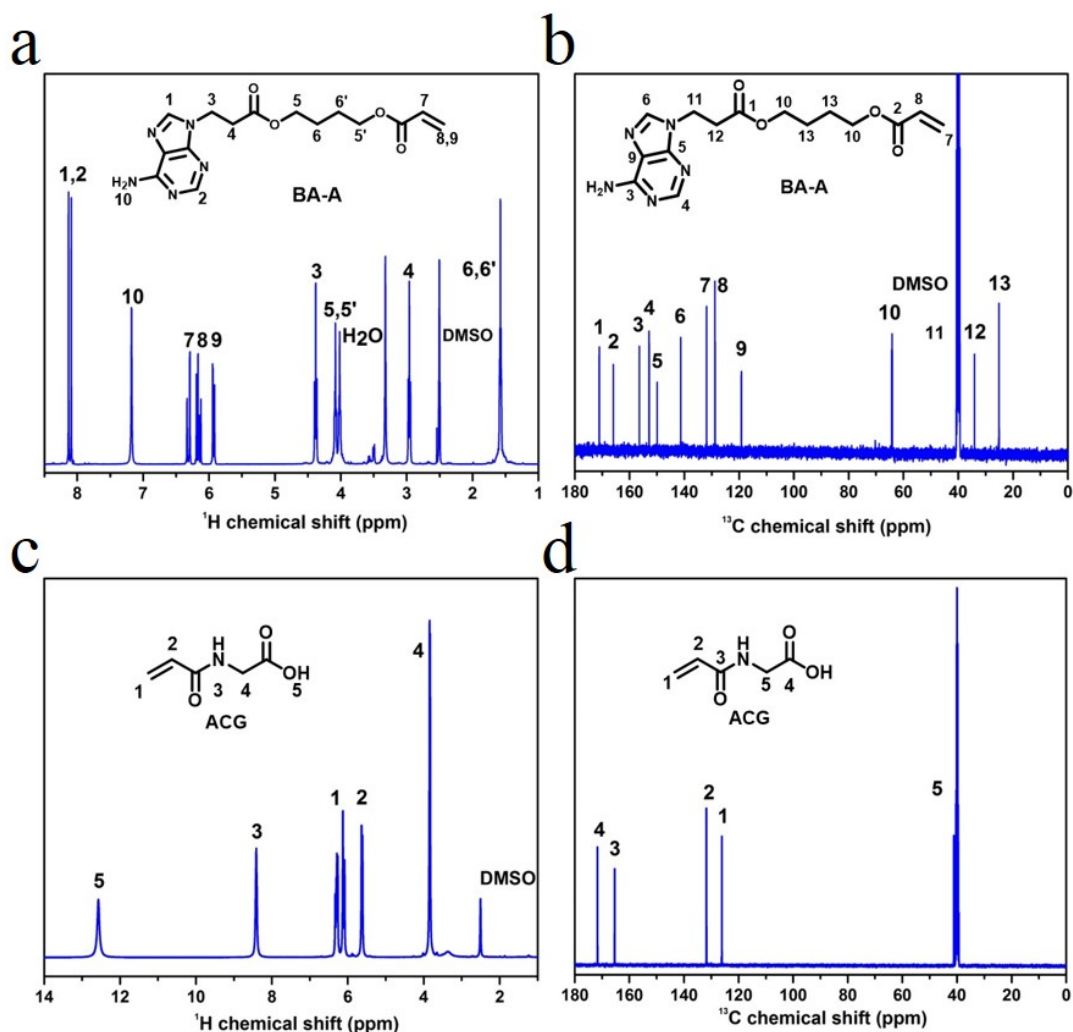


**Figure S1.**  $^1\text{H}$  NMR and  $^{13}\text{C}$  NMR spectra of BA-A, ACG (a) in  $\text{DMSO-d}_6$ .

$^1\text{H}$  NMR spectrum of BA-A ( $\text{DMSO-d}_6$ , 400 MHz): d 8.13–8.09 (d, 2H,  $\text{H}_{1+2}$ ), 7.15 (s, 2H,  $\text{H}_{10}$ ), 6.33–5.91 (m, 3H,  $\text{H}_{7+8+9}$ ), 4.38 (m, 2H,  $\text{H}_3$ ), 2.96 (m, 2H,  $\text{H}_4$ ), 4.08–4.02 (m, 4H,  $\text{H}_{5+5'}$ ), 1.57–1.59 (m, 4H,  $\text{H}_{6+6'}$ ) ppm.

$^{13}\text{C}$  NMR spectrum of BA-A ( $\text{DMSO-d}_6$ , 100 MHz,  $\delta$  ppm): 171.1, 165.9, 156.4, 152.6, 141.2, 131.9, 128.8, 119.1, 64.1, 33.9, 25.2.

$^1\text{H}$  NMR spectrum of ACG ( $\text{DMSO-d}_6$ , 400 MHz): d 6.1–6.3 (s, 2H,  $\text{H}_1$ ), 5.6 (s, 1H,  $\text{H}_2$ ), 8.4 (s, 1H,  $\text{H}_3$ ), 3.8 (s, 1H,  $\text{H}_4$ ), 12.6 (s, 1H,  $\text{H}_5$ ) ppm.

$^{13}\text{C}$  NMR spectrum of ACG ( $\text{DMSO-d}_6$ , 100 MHz,  $\delta$  ppm): 171.7, 165.5, 131.8, 126.4, 40.2

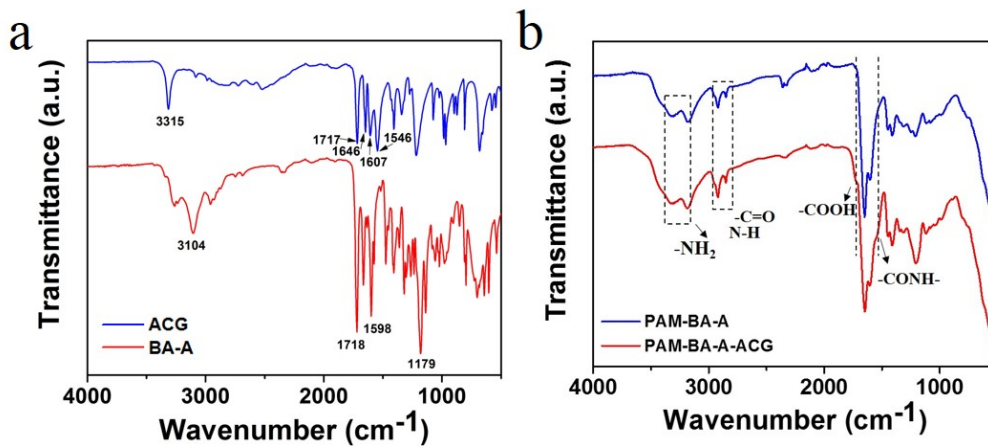


**Figure S2.** FTIR spectroscopy of ACG, BA-A, PAM-BA-A and PAM-BA-A-ACG hydrogels. In the spectrum of ACG, the peak appearing at  $1607\text{ cm}^{-1}$  was attributed to acryloyl C=C stretching, and the peaks at  $1646$  and  $1717\text{ cm}^{-1}$  were assigned to C=O stretching in amide and carboxyl groups, respectively; while signals from N-H bending and stretching appeared at  $1546$  and  $3315\text{ cm}^{-1}$  respectively. In the spectrum of BA-A, The absorption peak at  $3104\text{ cm}^{-1}$  was attributed to the stretching vibration peak of  $\text{-NH}_2$ , and the absorption peak at  $1718\text{ cm}^{-1}$  was attributed to the stretching vibration peak of  $\text{-C=O}$ , the peak appearing at  $1598\text{ cm}^{-1}$  was attributed to C=C stretching. It should be pointed out that the absorption peaks at  $1546\text{ cm}^{-1}$  were characteristic peaks of  $\text{-CONH-}$  of ACG. The peaks was in the polymer PAM-BA-A-ACG, but didn't not appear in the polymer PAM-BA-A without ACG involved in the reaction.

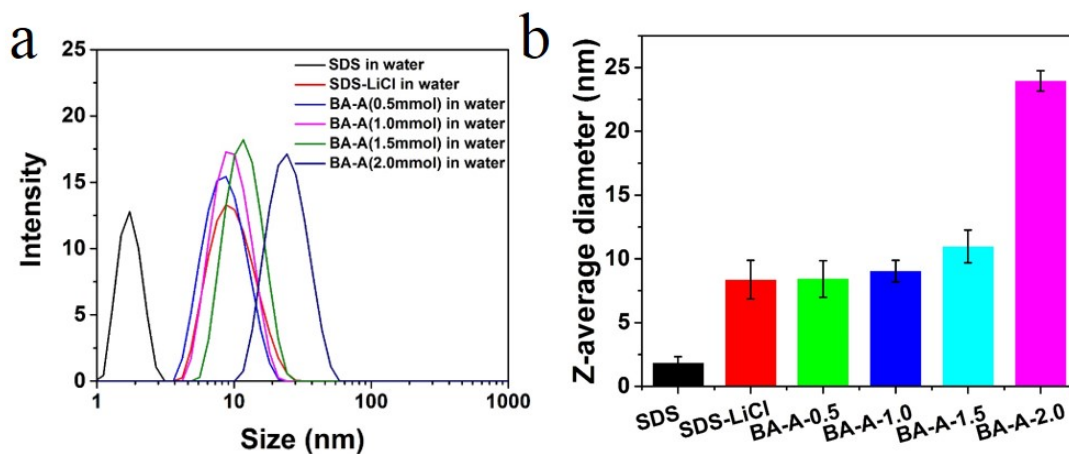


**Figure S3.** (a) Dynamic light scattering (DLS) spectra of SDS, SDS-LiCl, SDS-LiCl-BA-A and micellar solutions. (b) The Z-average diameter of SDS, SDS-LiCl, and SDS-LiCl-BA-A micellar solutions. As shown in Fig. S3, compared with the SDS micellar solution, the addition of lithium Chloride will cause the micelle particles grow from  $1.8 \pm 0.5\text{ nm}$  to  $8.3 \pm 1.5\text{ nm}$ . After the introduction of BA-A into SDS-LiCl micellar solution, it was found that the particle size increased to  $11.3 \pm 3.7\text{ nm}$  (BA-A-1.5 mmol). When monomer BA-A was 2 mmol, the particle size further increase to  $23.9 \pm 1.3\text{ nm}$ , indicating that BA-A can no longer be uniformly dispersed in the micellar solution.

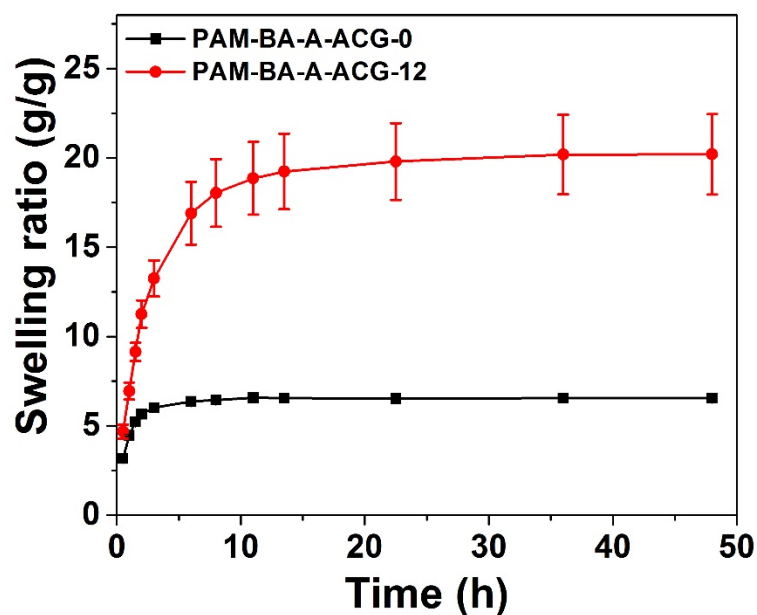


**Figure S4.** Swelling ratio of PAM-BA-A-ACG-0 and PAM-BA-A-ACG-12 hydrogels. As shown in Fig. S4, the addition of hydrophilic ACG monomer can effectively improve the swelling ratio of hydrogels, as the hydrogel reaches swelling equilibrium, the swelling rate of PAM-BA-A-ACG hydrogel is nearly three times that of PAM-BA-A hydrogel.

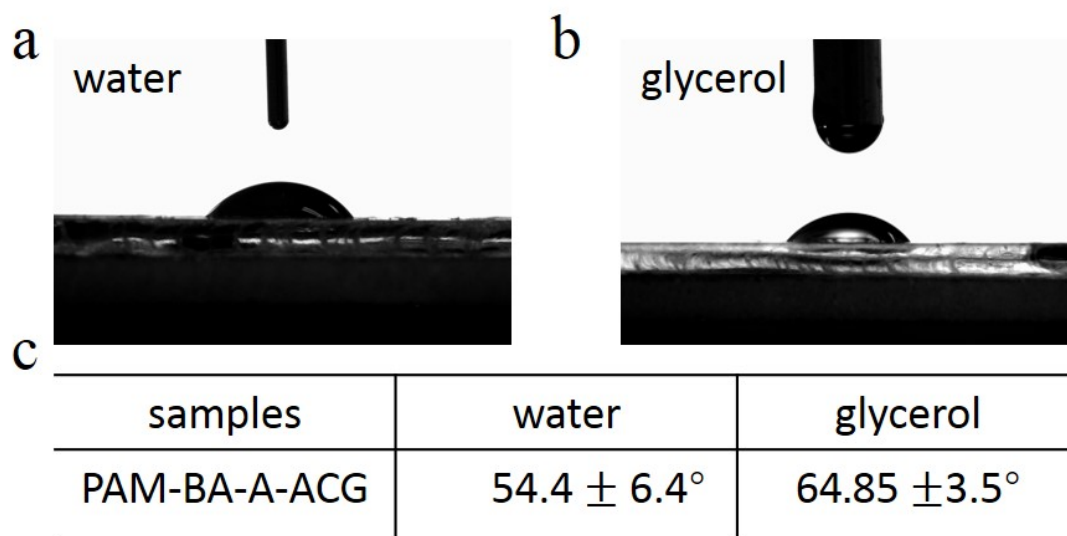


**Figure S5.** The images of (a) water drop and (b) glycerol drop on the PAM-BA-A-ACG hydrogel. (c) The results of contact angle measurement. The results showed that the water contact angle of the PDA-clay-PAM hydrogels was  $54.4 \pm 6.4^\circ$ , which indicated the hydrophilic nature of the hydrogels.

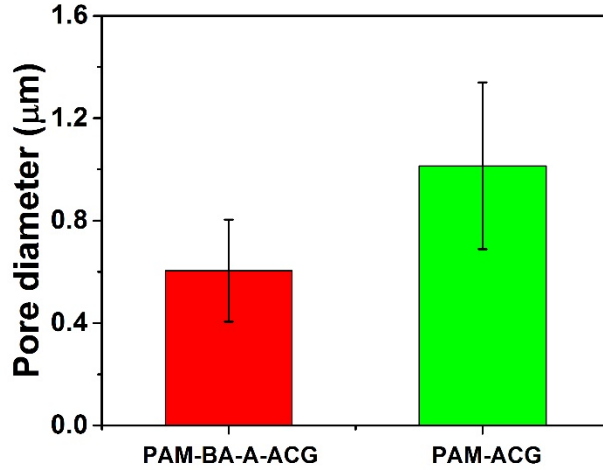


**Figure S6.** Pore size of PAM-BA-A-ACG and PAM-ACG hydrogels.

The average pore diameter of PAM-BA-A-ACG and PAM-ACG hydrogel was 0.6 μm, and 1.01 μm, respectively. The pore diameter of PAM-BA-A-ACG sample was smaller than PAM-ACG sample due to the nano-sized reinforcing domains by dynamic hydrogen bonds,  $\pi$ - $\pi$  stacking, and hydrophobic association interactions.

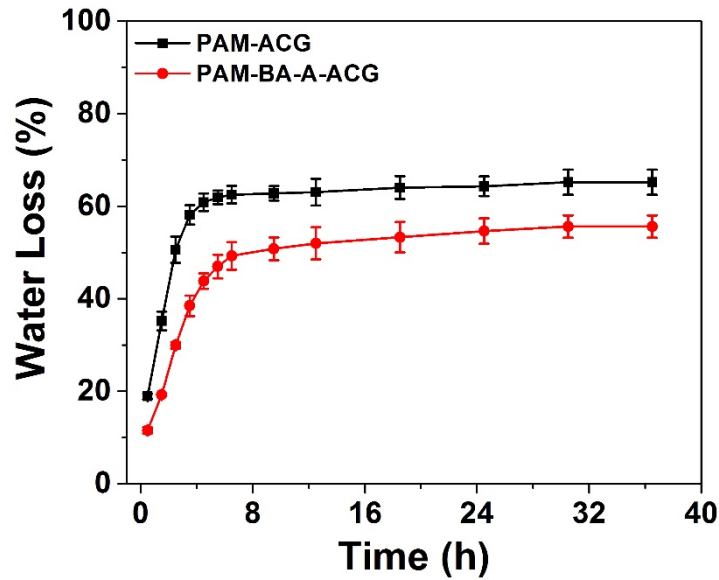


**Figure S7.** Evolutions of water loss with time for PAM-ACG and PAM-BA-A-ACG hydrogels kept in chamber with temperature of 25 °C and relative humidity of 20%.

To evaluate the accurate water loss of the hydrogels in the process, their masses were recorded every certain time using an electronic scale, and the water loss at time =  $i$  is calculated by<sup>1</sup>:

$$\text{Water Loss} = \left( \frac{\text{Mass}(\text{hydrogel}, \text{time} = i) - \text{Mass}(\text{hydrogel}, \text{time} = 0)}{\text{Mass}(\text{hydrogel}, \text{time} = 0)} \right) * 100\%$$

where Mass (water; time=0) is calculated by the amount of the raw materials used.

The water loss decreases from 65% to 55% as the addition of salts, indicating the effect of salt on the anti-drying property of hydrogels.

1. Y. Bai, B. Chen, F. Xiang, J. Zhou, H. Wang and Z. Suo, Transparent hydrogel with enhanced water retention capacity by introducing highly hydratable salt. *Appl. Phys. Lett.*, 2014, 105, 151903.